Spin-density-wave properties of $(Cr_{84}Re_{16})_{100-x}V_x$ alloys

BS Jacobs, ARE Prinsloo[1], CJ Sheppard and AM Strydom

Department of Physics, University of Johannesburg, PO Box 524, Auckland Park, 2006

E-mail address: alettap@uj.ac.za

Abstract. This paper reports on the spin-density-wave properties of the $(Cr_{84}Re_{16})_{100-x}V_x$ alloy system, with $0 \leq x \leq 10.4$ at.% V. The $Cr_{84}Re_{16}$ alloy represents an important and interesting position on the magnetic phase diagram of CrRe, just below the critical concentration where the Re concentration suppresses the antiferromagnetism in this alloy system. The possible coexistence of antiferromagnetism and superconductivity in CrRe was previously studied in samples with concentrations in the range of 14 to 25 at.% Re. In this study the $Cr_{84}Re_{16}$ alloy is tuned to a possible critical point through the addition of V. The Néel transition temperatures (T_N) for samples with x = 0, 5.7, 8.5 and 10.4 at.% V are obtained using electrical resistivity (ρ) and magnetic susceptibility (χ) measurements. A plot of T_N versus V concentration indicates the existence of a possible quantum critical point at $x \approx 10.5$ at.% V.

1. Introduction

The concentration versus temperature magnetic phase diagram of the CrRe alloy system exhibits three spin-density-wave (SDW) phases, the longitudinal (L) incommensurate (I) SDW, the transverse (T) ISDW and the commensurate (C) SDW [1]. A triple point is situated at $c_t \approx 0.30$ at.% Re, where the ISDW, CSDW and paramagnetic (P) phases coexist. Only a nearly linear ISDW–P phase line exists for $c < c_t$, but for $c > c_t$ both ISDW–CSDW and CSDW–P phase lines, which are strongly non-linear, appear on the phase diagram [1].

The CrRe system shows rather normal behaviour, fairly well understood within the framework of the canonical model, where Re behaves as an electron-donor in the Cr matrix [1]. As the Re concentration is increased above the triple point concentration, the electron and hole octahedral Fermi surfaces become closer in dimension. As both surfaces are almost of equal size, an improvement of the nesting of these two surfaces occurs with the concomitant increase in the Néel temperature (T_N) reaching saturation at ≈7 at.% Re. At about 7 at.% Re, perfect nesting between the electron and hole surfaces occurs [2, 3]. Higher concentrations of Re result in a reduction of T_N. This behaviour is presently not well understood, but corresponds to that observed for CrRu [1].

Previous research on CrRe has focussed on alloys and single crystals close to the triple point concentration [1, 4], as well as on concentrations in the range of 14 to 25 at.% Re [1]. Interest was drawn to CrRe alloys with concentrations above 14 at.% Re after the work of Muheim and Müller [5] on the nature of the phase boundary and the possible coexistence of the SDW and the superconducting phases in $Cr_{100-x}Re_x$ alloys, indicating superconductivity above 20 at.% Re. The coexistence of antiferromagnetism and superconductivity was found in a sample with 17 at.% Re [6], with a Néel temperature of approximately 160 K and superconducting transition temperature typically around 3 K. Superconductivity was also later found [7] in samples containing concentrations as low as 14 at.% Re,

with a superconducting transition of approximately 1 K. This research was extended by Nishihara *et al.* [8] investigating the magnetic and superconducting properties of samples containing between 14 to 25 at.% Re.

Due to severe metallurgical problems that can occur in preparing samples with uniform composition [5, 9], Damaschke and Felsch [7] however cautioned against the conclusion that the observation of a Néel transition in samples with concentrations higher than 14 at.% Re is used as firm evidence for the coexistence of the SDW and antiferromagnetic phases.

The behaviour around critical points of the Cr alloys can be probed by fine tuning of the parameters that influence SDW formation in these systems. The first such parameter is the effect of electron concentration on the area of the electron and hole Fermi surface sheets of Cr that nests [1] when the antiferromagnetic phase is entered. This nesting decreases the energy of the system through electron-hole pair condensation and results in the appearance of SDW energy gaps at the Fermi surface in certain directions of k-space on cooling through T_N. The nesting area, and concomitantly the stability of the SDW state, depends on the electron concentration per atom (*e/a*) which can easily be tuned by alloying Cr (*e/a* = 6) with elements like V (*e/a* = 5) or Mn (*e/a* = 7) to respectively decrease or increase the electron concentration. This effect plays a dominant role in affecting the SDW state in Cr alloys when alloyed with 3-d solutes that have an *e/a* number different from that of 3-d Cr. The second important parameter is the electron-hole pair breaking effect due to electron scattering by solute atoms. This parameter plays a dominant role when Cr is alloyed with the isoelectronic 4-d metals Mo (*e/a* = 6) or W (*e/a* = 6) [1] that leaves the electron concentration intact. Taking this into account there thus seems to be several options to tune $Cr_{100-x}Re_x$ through a critical point, using chemical doping with a third element as tuning parameter. This creates the opportunity to investigate the possibility of a quantum critical point in the CrRe alloy system, as well as the phase boundary between the antiferromagnetic and superconducting phase.

Utilizing the above mentioned characteristics Alberts *et al.* [10] investigated the magnetic and superconducting properties of $(Cr_{100-x}Mo_x)_{75}Ru_{25}$ with x = 0, 3, 6 and 10 at.% Mo. The results of this investigation was however inconclusive since these samples were superconducting, but none of them showed any evidence for the Néel transitions.

Recent work on CrRu [11, 12] reignited the interest in the CrRe alloy system, as much correspondence is seen between these two alloy systems [1]. Firstly, the *T-c* magnetic phase diagrams of these two systems are very similar and in the second place the possibility of the coexistence of the SDW phase together with the superconducting phase has also been considered in both these alloys previously [1]. The in-depth studies on $Cr_{86}Ru_{14}$ reported by Reddy *et al.* [11] resulted in investigations into the magnetic and quantum critical behaviour in a CSDW antiferromagnetic $(Cr_{86}Ru_{14})_{100-y}V_y$ system [12]. The concentration–temperature (y-T) magnetic phase diagram obtained for this system depicts a critical point at y = 10.4 at.% V, classified as a CSDW type of quantum critical point . This study indicated a peculiar difference in the mechanism responsible for driving this system and the $Cr_{100-z}Ru_z$ system to a quantum critical point using *e/a* as a tuning parameter. Our present work seeks to further illuminate this question.

The work by Reddy *et al.* [12] is strongly aligned with the current interest in quantum criticality in Cr alloy systems, as is reflected in recent literature [13, 14, 15, 16]. For a more comprehensive view, it is of interest to broaden studies on quantum criticality to a wider range of the different possible magnetic phase diagrams, and regions amenable to the quantum critical ground state of Cr alloy systems.

The present study is a preliminary investigation aiming to extend these studies to the CrRe system in order to better understand the quantum critical behaviour in Cr alloys in general.

2. Experimental

Pseudo-binary $(Cr_{84}Re_{16})_{100-x}V_x$, with $0 \leq x < 11$ at.% V alloys were prepared by arc melting in a purified argon atmosphere from 99.99 wt.% Cr, 99.99 wt.% Re and 99.8 wt.% V. The alloys were annealed in an ultra-high purity argon atmosphere at 1343 K for seven days and quenched into iced

water. Powder X-ray diffraction (XRD) analyses were used to confirm that the samples were single phase. The approximate chemical composition of the individual alloys was determined using a scanning electron microprobe (SEM) and energy-dispersive X-ray spectrometry (EDS). The actual elemental composition and homogeneity were determined using electron microprobe analyses. Electrical resistivity (ρ) and magnetic susceptibility (χ) were measured for $2 \leq T \leq 390$ K, using standard Physical Properties Measurement System (PPMS) incorporating appropriate measuring options and a Squid-type magnetometer based on the Magnetic Properties Measurement System (MPMS) platform of Quantum Design [17]. For magnetic susceptibility measurements the samples were cooled to 2 K in zero field and the measurements were done upon subsequent heating of the samples in a field of 100 Oe. Resistivity measurements for temperatures above 390 K were performed using resistive heating in an inert environment using the standard dc-four probe method and current reversal with Keithley instrumentation.

3. Results and discussion

The $Cr_{84}Re_{16}$ alloy represents an important and interesting position on the magnetic phase diagram of CrRe, just below the concentration where Re addition suppresses antiferromagnetism in this system and superconducting properties is also expected. By adding V to this alloy, the $(Cr_{84}Re_{16})_{100-x}V_x$ system can slowly be tuned to a critical point. In this way it is possible to investigate not only the phase boundary between the antiferromagnetic and superconducting phase, but also the possibility of a quantum critical point in this alloy system.

Special emphasis was placed on synthesizing specimens of high homogeneity and metallurgical quality in an effort to resolve magnetic and anticipated superconductivity instabilities and phase changes in the phase diagram of the system. This is of great importance as previous studies on CrRe pointed out severe metallurgical problems encountered in preparing samples of uniform composition [5, 9], attributed to the high vapor pressure of Cr at the liquidus temperature [1, 5]. The unusually high melting temperatures of refractory elements such as Re inevitably demands that adequate heat be supplied at the time of arc-melting in order to coerce full solution of the dopant elements into the Cr matrix. Figure 1 shows the xrd patterns for the $Cr_{84}Re_{16}$ sample. The entire profile in the $Cr_{84}Re_{16}$ spectra is well fitted to the xrd pattern of pure bcc Cr by adjusting the lattice parameter of pure Cr (2.8839 Å) to 2.9350 Å for this alloy, which corresponds well with that obtained previously in CrRe studies [18]. No additional peaks are detected to within instrumental resolution in the CrRe alloy spectra, indicating that the alloy formed in the bcc phase of pure Cr.

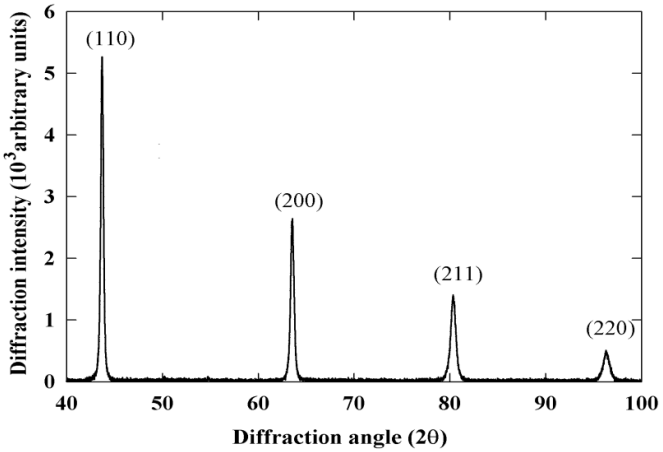

Figure 1. The xrd pattern for the $Cr_{84}Re_{16}$ sample with (hkl) Miller indices of the various reflections expected for the profile of bcc Cr indicated.

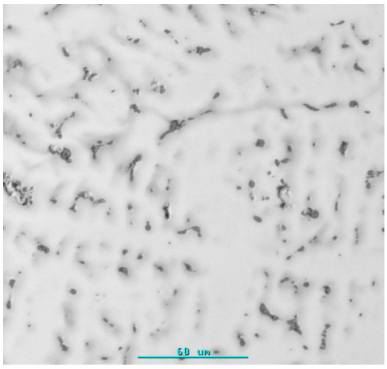

Figure 2. The backscattered-electron image of the $Cr_{84}Re_{16}$ alloy .

The backscattered-electron image of the $Cr_{84}Re_{16}$ annealed mother alloy is shown in figure 2. The image indicates that the mother alloy consists of a CrRe matrix with Cr concentration of (84±1) at.% and Re concentration of (16±1) at.%. Also clear in this image are dark spots. Wavelength dispersive X-ray spectra analyses showed the presence of oxygen within these dark inclusions. These inclusions cover approximately 3-4% of the image having a surface area of about 180μm^2. For the individual $(Cr_{84}Re_{16})_{100-x}V_x$ samples used in this study, the V concentrations were found to be 5.7, 8.5 and 10.4 at.%.

The $\rho(T)$ curves for $Cr_{84}Re_{16}$ and $(Cr_{84}Re_{16})_{100-x}V_x$, with x = 5.7, 8.5 and 10.4 at.% V, are shown in figure 3(a) and figure 3(b). A well defined anomaly in the form of a minimum is seen in the $\rho(T)$ curve of the $Cr_{84}Re_{16}$ sample, attributed to an induced SDW energy band gap at the Fermi energy on cooling through T_N [1]. T_N is often defined for Cr and its dilute alloys as the temperature of the minimum in $d\rho(T)/dT$ accompanying the magnetic phase transition [1]. This definition is also used for the present $(Cr_{84}Re_{16})_{100-x}V_x$ system. The inset in figure 3(a) depicts the temperature dependence of $d\rho(T)/dT$, obtained from the ρ-T curve of the mother alloy shown in figure 3(a), with the position of T_N marked by an arrow. The SDW anomaly is better defined in $d\rho(T)/dT$ than in $\rho(T)$ itself, especially for the alloys with higher V concentrations as an increase in the V concentration not only decreases the Néel temperature, but also results in a reduction in the size of the anomaly seen in these curves. T_N values obtained in this manner are plotted on the magnetic phase diagram of figure 5. The inset in figure 3(b) shows a weak low-temperature minimum for the $(Cr_{84}Re_{16})_{89.6}V_{10.4}$ sample, which is absent in the other three alloys. T_N for this sample was taken at the temperature associated with this minimum. The experimental error in the absolute value of ρ amounts to 5% and originates mainly from errors in determining the sample dimensions, while our instrumentation permitted a resistivity resolution of 0.5%. No evidence of superconductivity was seen in these samples down to 2K but measurements below 2 K are needed to clarify this issue.

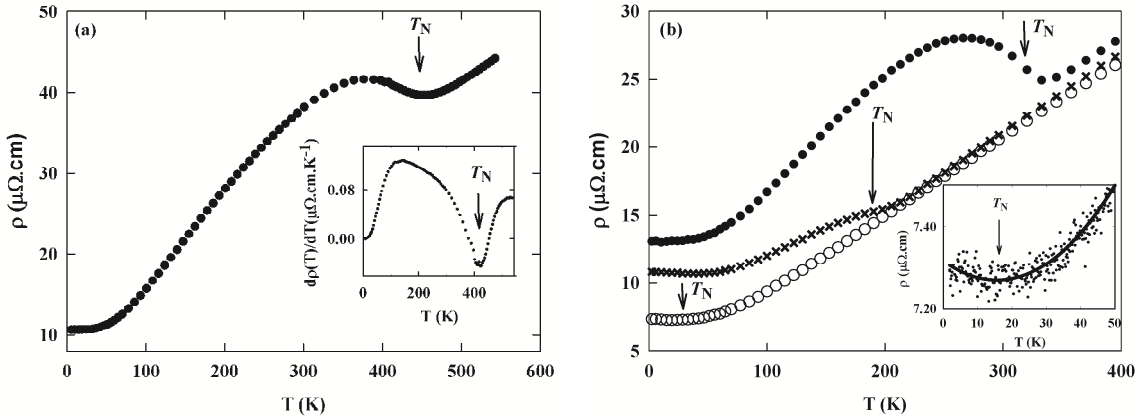

Figure 3. The temperature dependence of the electrical resistivity, ρ, of the (a) $Cr_{84}Re_{16}$ annealed mother alloy and (b) the $(Cr_{84}Re_{16})_{100-x}V_x$ alloys, with x = 5.7 (●) ,8.5 (×) and 10.4 (O) at.% V. The inset in (a) shows the temperature derivative ($d\rho(T)/dT$) of the $Cr_{84}Re_{16}$ alloy. The Néel temperatures (T_N) for the various samples, shown by arrows, are obtained from the minima of $d\rho(T)/dT$. The inset in (b) shows the weak minimum associated with T_N observed for the 10.4 at.% V sample and the line is a guide to the eye through the data.

The magnetic susceptibility (χ) as function of temperature for the samples containing 8.5 and 10.4 at.% V is shown in figures 4(a) and (b), respectively. In correspondence with results from previous studies [19] weak anomalies are seen in the χ-T curves, becoming more pronounced as the V concentration is increased. Although only a weak minimum was observed in the ρ-T curve of the

$(Cr_{84}Re_{16})_{89.6}V_{10.4}$ sample, a clear peak can be seen in the χ-T curve of this alloy giving $T_N \approx 28$ K. The Néel temperatures (T_N), shown by arrows in these figures, were obtained from the resistivity measurements. The transition temperatures from the χ-T curves were taken at the point where a decrease in χ occurs, as the antiferromagnetic phase is entered. The broken line in figure 4(a) is a fit to the data obtained in the paramagnetic phase, indicating the trend of the curve if the sample was to remain paramagnetic. T_N was taken at the point where the experimental values deviate from the broken line curve and the transition temperatures obtained in this manner correspond well with that determined from the $(d\rho(T)/dT)$ curves. T_N values obtained from the magnetic susceptibility measurements of the $(Cr_{84}Re_{16})_{100-x}V_x$ alloys with x = 5.7, 8.5 and 10.4 at.% V, were plotted on the magnetic phase diagram of figure 5. The transition temperature of the $Cr_{84}Re_{16}$ sample could however not be determined in the present MPMS setup, as it is limited to a maximum temperature of 400 K.

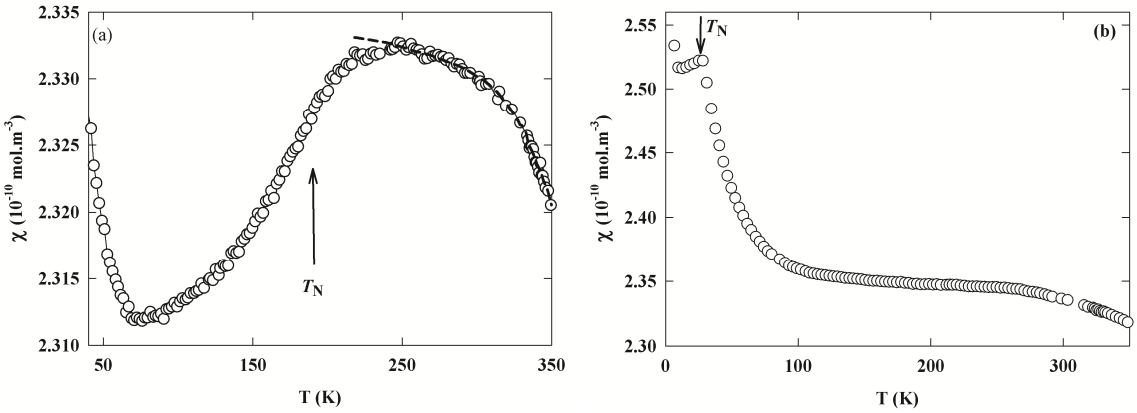

Figure 4. The temperature dependence of the magnetic susceptibily, χ, for the $(Cr_{84}Re_{16})_{100-x}V_x$ alloys, with (a) x = 8.5 and (b) 10.4 at.% V. The Néel temperatures (T_N), shown by arrows in these figures, are obtained from the resistivity measurements. The broken line in (a) is a fit to the experimental data in the paramagnetic region.

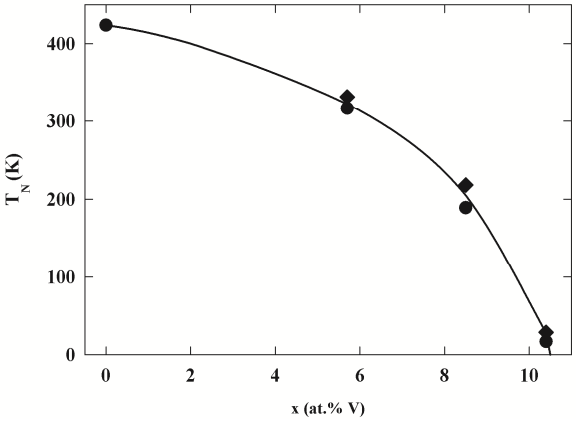

Figure 5. The magnetic phase diagram for the $(Cr_{84}Re_{16})_{100-x}V_x$ alloy system as a function of the V concentration, x, showing T_N values obtained through electrical resistivity (●) and magnetic susceptibility (◆) measurements. The error in the T_N values, obtained as explained in the text, falls within the size of the data points. The solid line is a guide to the eye.

Figure 5 shows the T_N values, obtained from the electrical resistivity and magnetic susceptibility measurements, as a function of V concentration for the samples investigated. The error in the T_N values falls within the size of the data points. The solid line is a guide to the eye through the data points. Extending the present results (see the figure for $x \geq 10.4$ at.% V) it seems that the SDW is suppressed down to 2 K at $x \approx 10.5$ at.% V. This suggests a possible quantum critical point at $x \approx 10.5$

at.% V. Measurements of additional physical properties are necessary in order to clarify this projection.

4. Conclusion.

The present study was devised to investigate the way in which antiferromagnetic ordering could be suppressed in the $(Cr_{84}Re_{16})_{100-x}V_x$ system. Our results are conducive to an interpretation of concentration-dependent magnetic ordering in this system, specifically through the addition of V as an electron dopant into the CrRe pseudo-binary alloy, and hence we conclude that a first and important ingredient of putative quantum criticality in this itinerant electron Cr system has been satisfied. Investigations are in progress to include more alloy concentrations, as well as, for example, Hall coefficient and magnetic susceptibility studies in order to explore the notion of criticality in this alloy system. These are frequently used parameters [15, 20, 21] used in assessing quantum critical behaviour in Cr alloy systems. Furthermore, measurements to temperatures below 2K are highly desirable for investigating the possibility of a superconducting dome at very low temperatures in the phase diagram.

Acknowledgements

This work was supported by the NRF of South Africa under Grant No. 2072956 and 61388.

References

[1] Fawcett E, Alberts HL, Galkin VY, Noakes DR and Yakhmi JV 1994 Rev. Mod. Phys. **66** 25
[2] Trego AL and Mackintosh AR 1968 Phys. Rev. **166** 495
[3] Arajs S, Moyer CA and Abukay D 1980 Phys. Stat. Sol. (b) **101** 63
[4] Boshoff AH, Alberts HL, Du Plessis P and Venter AM 1993 J. Phys.: Condens. Matter **5** 5353
[5] Muheim S and Müller J 1964 Phys. Kondens. Matter **2** 377
[6] Nishihara Y, Yamaguchi Y, Kohara T and Tokumoto M 1985 Phys. Rev. **B31** 5775
[7] Damaschke B and Felsch W 1986 Z. Phys. B **63** 179
[8] Nishihara Y, Yamaguchi Y, Tokumoto M, Takeda K and Fukamichi K 1986 Phys. Rev. **B34** 3446
[9] Kohara T, Asayama K, Nishihara Y and Yamaguchi Y, 1984 Solid State Commun. **49** 31
[10] Alberts HL, McLachlan DS, Germishuyse T and Naidoo M 1991 J. Phys.: Condens. Matter **3** 1793
[11] Reddy L, Alberts HL, Prinsloo ARE and Venter AM 2006 J. Alloys Comp. **426** 83
[12] Reddy L, Alberts HL, Strydom AM, Prinsloo ARE and Venter AM 2008 J. Appl. Phys. **103** 07C903-1
[13] Yeh A, Soh Y-A, J Brooke J, Aeppli G, Rosenbaum TF and Hayden SM 2002 Nature **419** 459
[14] Lee M, Husmann A, Rosenbaum TF and Aeppli G 2004 Phys. Rev. Lett. **92** 187201
[15] Jaramillo R, Feng Y, Wang J and Rosenbaum TF 2010 Proc. Nat. Acad. of Sci. USA (PNAS) **107** 13631
[16] Sheppard CJ, Prinsloo ARE, Alberts HL and Strydom AM 2011 J. Appl. Phys. **109**(7) 07E104
[17] Quantum Design Inc, 6325 Lusk Boulevard, San Diego, USA
[18] Nishihara Y, Yamaguchi Y, Waki S and Kohara T 1983 J. Phys. Soc. Japan **52**(7) 2301
[19] Arajs A, Kote G, Moyer CA, Kelly JR, Rao KV and Anderson EE 1976 Phys. Stat. Sol. (b) **74** K23
[20] Yeh A, Soh Y, Brooke J, Aeppli G and Rosenbaum TF 2002 Nature **419** 459
[21] Paschen S 2006 Physica **B378-380** 28